Academic Research Journal of Technical Vocational Schools, 1(1): 27-30 2022

Academic Research Journal of Technical Vocational Schools

| artes.cumhuriyet.edu.tr | Founded: 2022 Available online, ISSN: 2822-5880 Publisher: Sivas Cumhuriyet Üniversitesi

Effect of quantum barrier height on the linear and nonlinear optical properties of GaAs/AlGaAs Quantum Well

Didem Altun[1,2,a,*], **Kenan Altun**[3,b], **Behçet Özgür Alaydın**[1,3,c]

[1]Nanophotonic Application and Research Center, Sivas Cumhuriyet University, 58140, Sivas, Türkiye
[2]Department of Electricity and Energy, Sivas Vocational School of Technical Sciences, Sivas Cumhuriyet University, 58140, Sivas, Türkiye
[3]Department of Electronics and Automation, Sivas Vocational School of Technical Sciences, Sivas Cumhuriyet University, 58140, Sivas, Türkiye
*Corresponding author

Research Article

History

Received: 12/06/2022
Accepted: 28/06/2022

ABSTRACT

In this paper, we have considered the electronic and optical properties of $GaAs/Al_xGa_{1-x}As$ quantum well for different quantum barrier heights (QB). Under effective mass approximation, the finite element method is used to simulate wavefunctions and corresponding energy eigenvalues for two different quantum barrier heights in the absence of external fields. We have shown that except for the ground state, the first and second excited energy states have shifted up with increased QB heights which results in slight blue shifts in transition energies. It is shown that QB heights have no effect on the refractive index change of the (1-2) transition but the refractive index change of the (2-3) transition is decreasing with higher QB heights. In addition, it is seen that QB has a negligible effect on in absorption properties of both (1-2) and (2-3) transition but the intensity of the (2-3) transition is 2.5 times higher than (1-2) transition that makes (2-3) transition more suitable for any device application to have more efficient devices.

Keywords: Quantum well, linear and nonlinear optical properties, GaAs/AlxGa1-xAs, Quantum well, Quantum barrier

[a] *didemaltun@cumhuriyet.edu.tr* *https://orcid.org/0000-0002-1964-3538*
[c] *balaydin@cumhuriyet.edu.tr* *https://orcid.org/0000-0003-0935-4836*
[b] *kaltun@cumhuriyet.edu.tr* *https://orcid.org/0000-0001-7419-1901*

How to Cite: Altun D, Altun K, Alaydın BÖ, (2021). Effect of quantum barrier height on the linear and nonlinear optical properties of GaAs/AlGaAs Quantum Well, Academic Research Journal of Technical Vocational Schools, ??(?): ???-???

Giriş

IR emitting/absorbing devices have been studied extensively since the discovery of the potential use of IR radiation in many industrial, army and medical applications. Especially, semiconductor-based IR devices have been used a lot in the military, medical, and industrial fields in the last couple of decades (Wang, Slivken et al. 2021). One of the infrared devices used in this field is infrared sensors due to their frequent usage in night vision, tracking, and missile guidance (Harrer, Schwarz et al. 2016). Today infrared sensors have been taken up room in many fields such as health and communication due to the decrease in production costs (Vitiello, Scalari et al. 2015). Mercury-based materials are mostly used in infrared sensors, but working with this material group brings difficulties at the point of production (Hanna, Eich et al. 2016). In addition, infrared light sources are very rare and the intensity of infrared light have not been enough to be used in device till now. As an alternative to these materials, infrared sensors designed with GaAs/AlGaAs quantum wells have become popular optoelectronic materials in recent years to overcome these difficulties for infrared emitting/absorbing devices. GaAs/AlGaAs material group is not used only in infrared sensors, they are also used in infrared semiconductor lasers, and LEDs designed with quantum wells are among the common optoelectronic devices. In infrared semiconductor laser structures, which are widely used today, structures consisting of GaAs/AlGaAs multiple quantum wells are often used.

Quantum well structures are devices that operate based on transitions between minibands (Alaydin, Ozturk et al. 2017). The structure is created by selecting the appropriate well width and barrier height according to the region to be studied. In this way, it is possible to emit/detect infrared radiation with a certain wavelength. The reason why GaAs/AlGaAs is widely used in Quantum well structures is the excellent lattice compatibility between GaAs and AlAs, the direct bandgap of GaAs, and the relatively easy growth of these materials (Jiang, Xiao et al. 2018). The effects of external effects such as electric field, magnetic field, temperature, pressure, laser field on the optical and electronic properties of quantum wells are among important research topics (Karabulut et al., 2007; Karki et al., 2011; Ozturk, 2017; Alaydin, 2020; Durmuslar et al., 2021). Karabulut et al. (2007) studied the effect of laser field on the linear and nonlinear intersubband optical absorptions in an asymmetric rectangular quantum well (Karabulut, 2010). Yıldırım et al. analyzed the effect of Pöschl–Teller potential on nonlinear optical properties (Yıldırım and Tomak, 2005). Effects of temperature and hydrostatic pressure were shown for GaAs/InxGa1-xAs/GaAs square quantum well by Baser et al. (Baser et al., 2016). Alaydin showed the effects of quantum well thickness, quantum well barrier height and electric field for quantum cascade laser applications (Alaydin, 2020).

In this study, we have considered energy band structures of long-infrared emitting/absorbing GaAs/$Al_xGa_{1-x}As$ single quantum well heterojunction structure dependent on the quantum barrier height (QB) for quantum cascade laser/detector applications. Wavefunctions and corresponding energy eigenvalues were obtained by solving Schrödinger Equation using effective mass approximation. The finite element method was used to obtain solutions. Three bounded energy states were obtained and the probability density of wavefunctions, transitions energies, and dipole matrix elements was first calculated. Then, the changes in optical properties such as refractive index and absorption coefficient depending on the quantum barrier height were investigated to be used in long-infrared devices.

Theory and Method

The finite element method is one of the methods to find out the wave functions (WFs). Then corresponding energy levels (ELs) under effective mass approximation are simulated. Time-independent Hamiltonian of the GaAs/$Al_xGa_{1-x}As$ quantum well for different barrier heights is given in Equation (1) in matrix formalism,

$$H=-\frac{\hbar^2}{2m^*}\frac{d^2}{dz^2}+\frac{e^2 B^2 z^2}{2 m^* c^2}+e F z+V(z) \quad (1)$$

where the second-order differential is defined as Equation (2).

where m^* describes the effective mass of the electron it is taken as $0.067\ m_0$ due to lattice matching between GaAs and $Al_xGa_{1-x}As$ (m_0 is the free electron mass). In equation 1, e is the electron charge, N_z is the length of the matrix to define the total quantum region, F is the electric field in the growth direction, B is the magnetic field applied perpendicular to the growth direction, and $V(z)$ is the confinement potential. The quantum well is 15 nm thick and it is surrounded by the $Al_xGa_{1-x}As$ quantum barrier. V_0 is the band discontinuity and it is taken as 0.6. Quantum barrier height is taken as V_0 =290 meV for $x = 0.45$ (V_0 =228 meV for $x = 0.3$,) [1, 2].

The diagonalization method is used to calculate Equation (1). Energy levels are obtained and then their corresponding electron wavefunctions (WFs), linear absorption coefficients (LACs), third-order nonlinear absorption coefficients (NACs), and total absorption coefficients (TACs) are simulated for intersubband (ISB) transitions for the three ELs. The density matrix approach as given in Equation (3) is used.

$$\frac{d^2}{dz^2}=\left[-2\,\mathrm{diag}\left(\mathrm{ones}(1,N_z)\right)+\mathrm{diag}(\mathrm{ones}(1,N_z-1),-1)+\mathrm{diag}(\mathrm{ones}(1,N_z-1),1)\right]^2 \quad (2)$$

$$\beta_{if}^{(1)}(\omega)=\omega\sqrt{\frac{\mu}{E_r}}|M_{if}|^2\frac{e^2\sigma_v\hbar\Gamma}{(E_{if}-\hbar\omega)^2+(\hbar\Gamma)^2} \quad (3)$$

$$\beta_{if}^{(3)}(\omega,I)=-2\omega\sqrt{\frac{\mu}{E_r}}|M_{if}|^4\left(\frac{I}{E_0 c\, n_r}\right)\frac{e^4\sigma_v\hbar\Gamma}{\{(E_{if}-\hbar\omega)^2+(\hbar\Gamma)^2\}^2}\times\left[1-\frac{|\delta_{if}|^2}{|2M_{if}|^2}\left(\frac{(E_{if}-\hbar\omega)^2-(\hbar\Gamma)^2+2E_{if}(E_{if}-\hbar\omega)}{(E_{if})^2+(\hbar\Gamma)^2}\right)\right] \quad (4)$$

$$\beta_{if}(\omega,I)=\beta_{if}^{(1)}(\omega)+\beta_{if}^{(3)}(\omega,I) \quad (5)$$

The LRICs, NRICs, and TRICs can be formulated as (3), respectively.

$$\frac{\Delta n_{if}^{(1)}(\omega)}{n_r}=\frac{e^2\sigma_v}{2E_0 n_r^2}|M_{if}|^2\frac{(E_{if}-\hbar\omega)}{(E_{if}-\hbar\omega)^2+(\hbar\Gamma)^2} \quad (6)$$

$$\frac{\Delta n_{if}^{(3)}(\omega,I)}{n_r}=-\frac{\mu c}{4E_0 n_r^3}|M_{if}|^2\frac{e^4\sigma_v I}{\{(E_{if}-\hbar\omega)^2+(\hbar\Gamma)^2\}^2}\times\left[4(E_{if}-\hbar\omega)|M_{if}|^2-\frac{{\delta_{if}}^2}{(E_{if})^2+(\hbar\Gamma)^2}\times\{(E_{if}-\hbar\omega)[E_{if}(E_{if}-\hbar\omega)-(\hbar\Gamma)^2]-(\hbar\Gamma)^2[2E_{if}-\hbar\omega]\}\right] \quad (7)$$

$$\frac{\Delta n_{if}(\omega,I)}{n_r}=\frac{\Delta n_{if}^{(1)}(\omega)}{n_r}+\frac{\Delta n_{if}^{(3)}(\omega,I)}{n_r} \quad (8)$$

Intersubband dipole moment matrix elements (DMMEs) are defined by

$$M_{if}=\int\Psi_f^*\,z\,\Psi_i\,dz,\qquad (i,f=1,2,3,4) \quad (9)$$

Here, $\delta_{if} = M_{ff} - M_{ii}$ is the intrasubband DMMEs, I is the optical light intensity, ω is the angular frequency of the incident photon, $(E_{if} = E_f - E_i = \hbar\,\omega_{if})$, E_f and E_i represent the quantized ELs for the last and first states, $\mathcal{E}_0$ is the vacuum permittivity, $\mathcal{E}_r$ is the real part of the permittivity, μ is the magnetic permeability, n_r is the refractive index, σ_v is the carrier density.

Result and Discussion

We have theoretically investigated the electronic and optical features for the (1-2) and (2-3) transitions in the square quantum well dependent on the QB (electric (F) and magnetic (B) fields are not included. In this study, we have taken $\sigma_v = 4 \times 10^{16} \mathrm{cm}^{-3}$, $T = 1 / \Gamma = 0.14$ ps [3-5] and I is $0.2\ \mathrm{MW/cm^2}$. In Figure 1, band arrangement is shown. It has been seen that QB height has minor effect on the eigenvalue of the ground energy state. In addition, localization and its shape are also not affected. It is calculated that transition energies (1-2) and (2-3) are 50 meV and 79 meV which are in THz region. When QB height is increased to 290 meV, there are slight increase in transition energies that are respectively 52 meV and 84 meV. These values are in THz region and also suitable for semiconductor devices working in THz region.

Refractive index change of the (1-2) and (2-3) transitions are given in Figure 2. LACs, NACs and TACs are plotted for different QB heights. It is seen that linear refrative index change is stronger than perturpative nonlinear refractive index change under current band arrangenements and parameters for both QB heights. There is a negligible change in the refractive index change of the (1-2) transition dependent on the QB heights. However, TAC of the (2-3) transition is higher for the lower QB height owing to the stronger NAC of the higher QB height. We can say that QB height results in higher perturbative effect for (2-3) transition.

Figure 3 depicts the absorption properties square QW dependent on the different QB heights. The same as the refractive index change absorption coefficients of the (1-2) transition is not affected from QB height due to same dipole moment matrix elements. As described in equation 5 and 6, absorption coefficient is function of the dipole moment matrix elements and incident intensity. Non-changing behavior of the ground state wavefunctions and slightly varying first excited state are the defining factor. Absorption coefficients of the (2-3) transitions are 2.5 times higher than (1-2) transition that indicates more efficient device operation if designed for (2-3). However, slight change observed in refractive index change is not observable for the different QB barrier height.

Conclusion

As a conclusion, we have studied the electro-optical properties of GaAs/$Al_xGa_{1-x}As$ square quantum well for different QB heights. The first three bounded energy levels for (1-2) and (2-3) intrasubband transitions are considered. Ground state energy is not affected by the variation of the QB height. However, energy eigenvalues are shifting up with QB height for excited state and blue shift is observed in transition energies. We have observed that refractive index of the (1-2) transition is independent from the QB height but refractive index of the (2-3) transition is varying with QB height. Refractive index change is in the same order for the (1-2) and (2-3) transition. Calculated absorption coefficients show that (2-3) transition is more effective than (1-2) transition. Any device design based on (2-3) transition will be more efficient than (1-2) due to higher overlap of the PDWs. Lastly, we think that the current study can contribute design and research of QW semiconductor devices such as photodetectors, lasers, semiconductor saturable absorbers by showing the way how design optical properties.

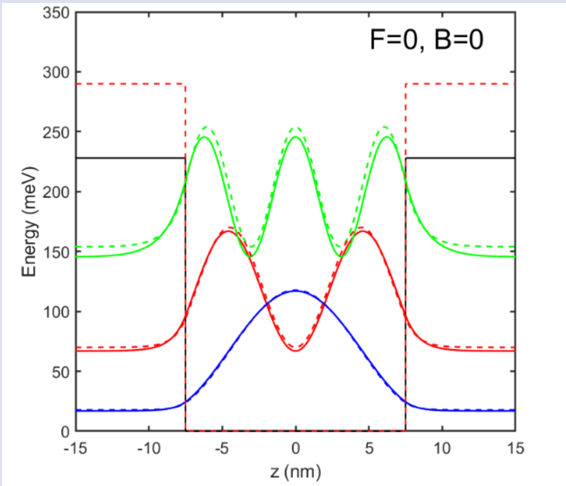

Figure 1. PDWs of first three energy states in the conduction band of QW structure in the for different quantum well barrier heights

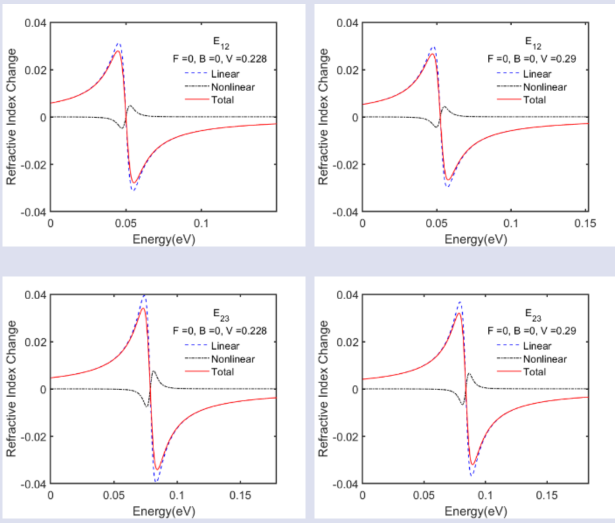

Figure 2. Absorption coefficents of the (1-2) and (2-3) transitions for different square quantum well barrier heights

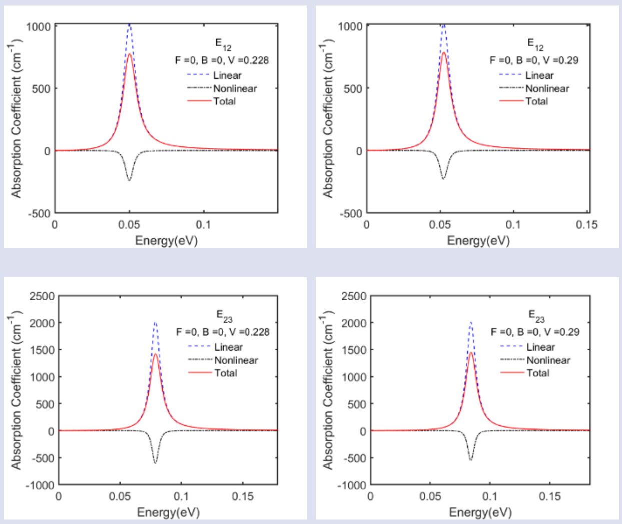

Figure 3. Absorption coeffients of the (1-2) and (2-3) transitions for different square quantum well barrier heights.

References

Alaydin B. O. (2020). Effect of high bandgap AlAs quantum barrier on electronic and optical properties of In0.70Ga0.30As/Al0.60In0.40As superlattice under applied electric field for laser and detector applications. International Journal of Modern Physics B 35(02): 2150027.

Alaydin B. O., Ozturk E. and Elagoz S. (2017). Interband transitions dependent on indium concentration in Ga1−xInxAs/GaAs asymmetric triple quantum wells. International Journal of Modern Physics B 32(05): 1850052.

Baser P., Altuntas I, Elagoz S. (2016). The hydrostatic pressure and temperature effects on hydrogenic impurity binding energies in GaAs/InxGa1-xAs/GaAs square quantum well. Microstructures. 92: 210-216.

Durmuslar A. S., Billur C. A., Turkoglu A. and Ungan F. (2021). Optical properties of a GaAs quantum well with new type of hyperbolic confinement potential: Effect of structure parameters and intense laser field. Optics Communications 499: 127266.

Hanna S., Eich D., Mahlein K. M., Fick W., Schirmacher W., Thöt R., Wendler J. and Figgemeier H. (2016). MCT-Based LWIR and VLWIR 2D Focal Plane Detector Arrays for Low Dark Current Applications at AIM. Journal of Electronic Materials 45(9): 4542-4551.

Harrer A., Schwarz B., Schuler S., Reininger P., Wirthmüller A., Detz H., MacFarland D., Zederbauer T., Andrews A. M., Rothermund M., Oppermann H., Schrenk W. and Strasser G. (2016). 4.3 μm quantum cascade detector in pixel configuration. Optics Express 24(15): 17041-17049.

Jiang M., Xiao H. Y., Peng S. M., Yang G. X., Liu Z. J. and Zu X. T. (2018). A comparative study of low energy radiation response of AlAs, GaAs and GaAs/AlAs superlattice and the damage effects on their electronic structures. Scientific Reports 8(1): 2012.

Karabulut I. (2010). Laser field effect on the nonlinear optical properties of a square quantum well under the applied electric field. Applied Surface Science 256(24): 7570-7574.

Karabulut İ., Atav Ü., Şafak H. and Tomak M. (2007). Second harmonic generation in an asymmetric rectangular quantum well under hydrostatic pressure. Physica B: Condensed Matter 393(1): 133-138.

Karki H. D., Elagoz S. and Baser P. (2011). The high hydrostatic pressure effect on shallow donor binding energies in GaAs–(Ga, Al)As cylindrical quantum well wires at selected temperatures. Physica B: Condensed Matter 406(11): 2116-2120.

Ozturk E. (2017). Depending on the electric and magnetic field of the linear optical absorption and rectification coefficient in triple quantum well. Optical and Quantum Electronics 49(8): 270.

Vitiello M. S., Scalari G., Williams B. and De Natale P. (2015). Quantum cascade lasers: 20 years of challenges. Optics Express 23(4): 5167-5182.

Wang F., Slivken S. and Razeghi M. (2021). High-brightness LWIR quantum cascade lasers. Optics Letters 46(20): 5193-5196.

Yıldırım H. and Tomak M. (2005). Nonlinear optical properties of a Poschl-Teller quantum well. Physical Review B 72(11): 115340.